PROCEEDINGS OF SCIENCE

Lepton universality in semileptonic b decays with τ leptons at LHCb

Luke George Scantlebury-Smead[†,*]

University of Oxford,
Parks Rd, Oxford, United Kingdom

E-mail: luke.george.scantlebury.smead@cern.ch

In the Standard Model, the coupling of the electroweak gauge bosons to each of the three charged leptons is identical. Recent measurements have shown hints that this principle may be violated, and may be due to new physics phenomena. The lepton universality tests performed with semileptonic b decays with τ leptons by LHCb are presented and future prospects are discussed.

11th International Workshop on the CKM Unitarity Triangle (CKM2021)
22-26 November 2021
The University of Melbourne, Australia

[†]on behalf of the LHCb collaboration.
[*]Speaker

PoS(CKM2021)067

1. Introduction

In the Standard Model (SM) the electroweak coupling to each of the three charged leptons is identical, which means that transition rates involving these leptons are expected to be the same up to phase-space effects related to the lepton mass. This principle is known as Lepton Flavour Universality (LFU). Many of the tests of LFU that have been performed involve the measurement of the ratio of branching fractions of decays with final states differing by lepton flavour, for semileptonic b decays with τ leptons: $\mathcal{R}(X_c) \equiv \frac{\mathcal{B}(X_b \to X_c\,\tau^+\,\nu_\tau)}{\mathcal{B}(X_b \to X_c\,\mu^+\,\nu_\mu)}$, where X_b and X_c are b- and c-hadrons, respectively [1]. The tree level $b \to c\ell\nu_\ell$ transition provides many tests of LFU; three such tests performed by LHCb using the LHCb Run 1 data, corresponding to an integrated luminosity of 3 fb^{-1}, are presented here. A measurement of $\mathcal{R}(J/\psi)$ is presented, where the muonic τ decay is used, and two measurements of $\mathcal{R}(D^*)$ are presented, one using the muonic τ decay, and the other using the three-pronged hadronic τ decays, $\tau^+ \to \pi^+\pi^-\pi^+(\pi^0)\overline{\nu}_\tau$.

2. $\mathcal{R}(D^*)$ hadronic

The hadronic measurement of $\mathcal{R}(D^*)$ with three-pronged τ decays is performed using a prompt normalisation channel. In this way, $\mathcal{R}(D^*)$ is measured as $\mathcal{R}(D^*) = \mathcal{K}(D^*)\frac{\mathcal{B}(B^0 \to D^{*-}3\pi^\pm)}{\mathcal{B}(B^0 \to D^{*-}\mu^+\nu_\mu)}$ where $\mathcal{K}(D^*) = \frac{\mathcal{B}(B^0 \to D^{*-}\tau^+\nu_\tau)}{\mathcal{B}(B^0 \to D^{*-}3\pi^\pm)}$ [2, 3]. The normalisation was chosen due to it having the same final state as the signal decay, since the neutrinos in the B^0 and τ^+ decays are not reconstructed and the $\tau^+ \to \pi^+\pi^-\pi^+(\pi^0)\overline{\nu}_\tau$ decays are used to partially reconstruct the τ. The $D^{*-} \to (\overline{D}^0 \to K^+\pi^-)\pi^-$ decay is used to fully reconstruct the D^{*-} meson. The prompt $B \to D^{*-}3\pi^\pm X$ decays are the most abundant background in the analysis with approximately 100 times more events that the signal mode. These decays are heavily suppressed by requiring the 3π and B^0 vertex z-axis separation to be greater than 4 times its uncertainty. Remaining backgrounds include $B \to D^{*-}(D_s^+,\, D^+,\, D^0)X$ double-charm decays which have a similar decay topology to the signal due to the non-negligible life time of the charm mesons, and $B \to D^{**}\tau^+\nu_\tau$ feed-down decays which are assumed to constitute $11.0 \pm 4.4\%$ of the signal yield.

A three-dimensional binned template fit is used to measure the signal yield, using τ^+ decay time, $q^2 = |P_{B^0} - P_{D^*}|^2$, and the output of a Boosted Decision Tree (BDT) which is used to discriminate signal and $B \to D^{*-}DX$ decays. The one-dimensional projections of the three fit variables are shown in Figure 1. This analysis measures $\mathcal{R}(D^*) = 0.291 \pm 0.019(\text{stat}) \pm 0.026(\text{sys}) \pm 0.013(\text{ext})$ where the third uncertainty is due to the limited knowledge of the $B^0 \to D^{*-}\mu^+\nu_\mu$ and $B^0 \to D^{*-}3\pi^\pm$ branching fractions. This measurement has a 12% precision, is 1.1σ above the Standard Model, and is compatible with the experimental average. The largest systematic uncertainty for this measurement arises from the finite size of the simulation samples used. This is followed by uncertainties related to the double-charm backgrounds. Future analyses will benefit from fast simulation developments which will increase the simulation to data ratio [4]. Additionally, recent measurements of background modes will increase knowledge of the double-charm backgrounds, such as the angular analysis of $B^0 \to D^{*-}D_s^{*+}$ [5].

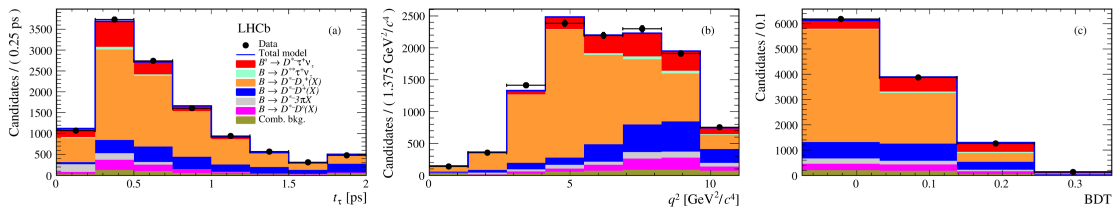

Figure 1: The one-dimensional projections of τ^+ decay time (left), q^2 (middle), and BDT output (right) for the $\mathcal{R}(D^*)$ hadronic signal data. The projections of the fit model are also shown.

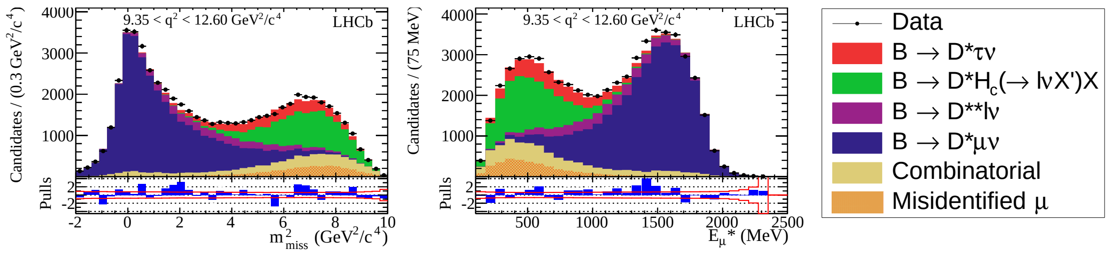

Figure 2: The one-dimensional projections of m^2_{miss} (left) and E^*_μ (middle) in the highest q^2 bin, $(9.35 < q^2 < 12.60\,\text{GeV}^2/c^4)$, for the $\mathcal{R}(D^*)$ muonic signal data. The projections of the fit model are also shown and a legend (right) is provided.

3. $\mathcal{R}(D^*)$ muonic

The muonic $\mathcal{R}(D^*)$ measurement is able to measure $\mathcal{R}(D^*) = \frac{\mathcal{B}(B^0 \to D^{*-}\tau^+\nu_\tau)}{\mathcal{B}(B^0 \to D^{*-}\mu^+\nu_\mu)}$ directly; there is no need for an intermediate normalisation mode since the τ and μ modes have the same final state, $D^{*-}\mu^+$ [6]. As in the hadronic analysis, the $D^{*-} \to (\overline{D}^0 \to K^+\pi^-)\pi^-$ decay is used. Neither decay can be fully reconstructed due to missing neutrinos, however, the B^0 momentum can still be approximated. The component of the B^0 momentum along the beam axis is approximated with $(p_{B^0})_z = (m_{B^0}/m_{\text{reco}})(p_{\text{reco}})_z$, where m_{B^0} is the known B^0 mass and m_{reco} and $(p_{\text{reco}})_z$ are the mass and momentum of the reconstructed $D^{*-}\mu^+$ system. The τ and μ decay modes are selected in the same sample using a BDT to reduce backgrounds with additional charged tracks and are then separated using a three-dimensional binned template fit to the variables $q^2 = |P_{B^0} - P_{D^*}|^2$, $m^2_{\text{miss}} = (P_{B^0} - P_{D^*} - P_\ell)^2$, and E^*_μ which is the μ energy in the B^0 rest frame.

The final sample obtained contains several backgrounds, $B \to D^{*-}H_cX$, where H_c undergoes a semileptonic decay, $B \to D^{**}\tau\nu_\tau$, $B \to D^{**}\mu\nu_\mu$, random track combination events, and events where hadrons are misidentified as μ. The templates for the signal and background components are taken from simulation and control samples and are used to measure the yields of each component. The one-dimensional projections of m^2_{miss} and E^*_μ in the highest q^2 bin are shown in Figure 2. This analysis measures $\mathcal{R}(D^*) = 0.336 \pm 0.027(\text{stat}) \pm 0.040(\text{sys})$ which has a 14% precision and is 1.7σ above the SM prediction. The largest systematic uncertainty for this measurement is due to the finite size of the simulation samples used, followed by the uncertainty due to the misidentified μ template shape. The systematic from the misidentified μ template shape can be reduced in future analyses with improved rejection of this background and more sophisticated modelling. Additionally, particle identification calibration samples with a broader momentum range and less trigger bias, created after this measurement was made, will reduce the uncertainty from this background.

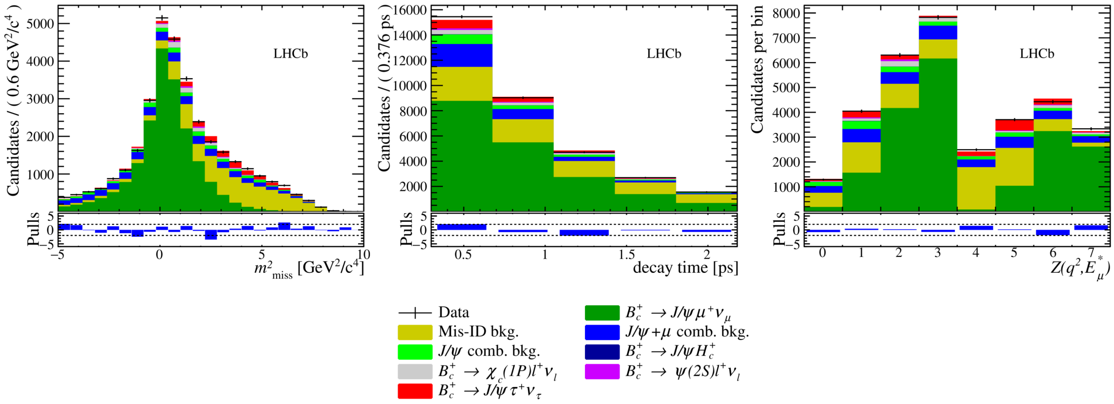

Figure 3: The one-dimensional projections of m^2_{miss} (left), B_c^+ decay time (middle), and Z (right) for the $\mathcal{R}(J/\psi)$ muonic signal data. The projections of the fit model are also shown and a legend is provided.

4. $\mathcal{R}(J/\psi)$ muonic

The $\mathcal{R}(J/\psi)$ muonic measurement is able to measure $\mathcal{R}(J/\psi) = \frac{\mathcal{B}(B_c^+ \to J/\psi\tau^+\nu_\tau)}{\mathcal{B}(B_c^+ \to J/\psi\mu^+\nu_\mu)}$ directly since both the τ and μ decays have the same visible final state [7]. The signal yields are extracted from the signal data sample through a three-dimensional binned template fit to the variables m^2_{miss}, B_c^+ decay time, and a composite variable Z. The variable Z is constructed by flattening a two-dimensional histogram of q^2 and E^*_μ, where q^2 is split into two bins ($q^2 < 7.15$ GeV$^2/c^4$ and $q^2 \geq 7.15$ GeV$^2/c^4$), and E^*_μ is divided into four bins with thresholds of $[0.68, 1.15, 1.64]$ GeV. The largest background in the final signal sample is composed of events where hadrons are misidentified as μ, but other backgrounds are present such as random track combination events, $B_c^+ \to \chi_c(1P)\ell^+\nu_\ell$, and $B_c^+ \to \psi(2S)\ell^+\nu_\ell$. The one-dimensional fit projections for m^2_{miss}, B_c^+ decay time, and Z are shown in Figure 3 and a value of $\mathcal{R}(J/\psi) = 0.71 \pm 0.17(\text{stat}) \pm 0.18(\text{sys})$ is obtained. Evidence of the $B_c^+ \to J/\psi\tau^+\nu_\tau$ decay is also observed for the first time, at a significance of 4.7σ. The measured value of $\mathcal{R}(J/\psi)$ has a precision of 35% and is 2σ above the SM value.

5. Conclusion and prospects

Several deviations from the SM are observed in LFU tests using $b \to c\ell\nu_\ell$ transitions at LHCb. The combination of the hadronic and muonic $\mathcal{R}(D^*)$ measurements is 2.1σ above the SM, while the muonic $\mathcal{R}(J/\psi)$ measurement is 2σ above the SM. When including other measurements of $\mathcal{R}(D^*)$ as well as $\mathcal{R}(D)$, the global average is 3.4σ above the SM, as seen in Figure 4. The results presented here use the LHCb Run 1 dataset, but several updates are underway, using either LHCb Run 2 data, or the full LHCb Run 1 + Run 2 dataset. These larger datasets, along with the previously mentioned improvements to fast simulation techniques, will significantly improve statistical and systematic uncertainties in these measurements. Precision measurements of large background modes will also reduce the systematic uncertainties associated with these backgrounds. In addition to updates to these presented analyses, several $\mathcal{R}(X_c)$ analyses are underway, such as $\mathcal{R}(D^0)$, $\mathcal{R}(D^+)$, $\mathcal{R}(D_s^+)$, and $\mathcal{R}(\Lambda_c^+)$. Decays involving $b \to u\ell\nu_\ell$ transitions are also being investigated, such as $\Lambda_b^0 \to p\tau^-\overline{\nu}_\tau$ and $B^+ \to p\overline{p}\tau^+\nu_\tau$.

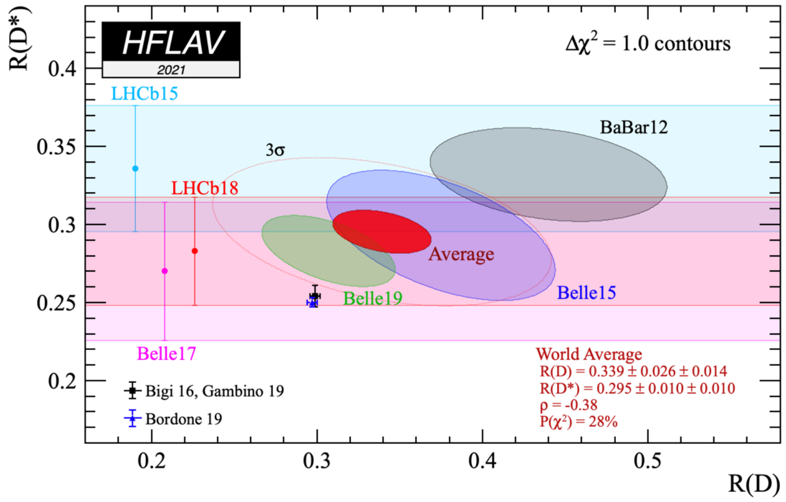

Figure 4: The global average of $\mathcal{R}(D)$ and $\mathcal{R}(D^*)$ measurements, performed by the Heavy Flavour Averaging Group [1]. The red ellipse shows the 1σ region of the global average and SM predictions are shown with the blue and black markers.

Angular analyses will also expand the tests of LFU available for these modes by providing additional observables beyond decay rate measurements. Using angular observables, different NP models can be distinguished, and NP can be detected even if $\mathcal{R}(D^*)$ becomes compatible with the SM predictions. A longitudinal D^* polarisation measurement in $B^0 \to D^{*-}\tau^+\nu_\tau$ decays is underway as well as other angular analyses that measure additional observables. One proposed method uses the HAMMER package to reweight SM simulation to arbitrary NP Wilson coefficients and form factors in order to measure them [8]. Another method developed is model independent, and measures the twelve angular coefficients with no form factor assumptions [9].

References

[1] Y. S. Amhis *et al.*, "Averages of b-hadron, c-hadron, and τ-lepton properties as of 2018," *Eur. Phys. J.*, vol. C81, p. 226, 2021. updated results and plots available at `https://hflav.web.cern.ch/`.

[2] R. Aaij *et al.*, "Measurement of the ratio of the $B^0 \to D^{*-}\tau^+\nu_\tau$ and $B^0 \to D^{*-}\mu^+\nu_\mu$ branching fractions using three-prong τ-lepton decays," *Phys. Rev. Lett.*, vol. 120, p. 171802, Apr 2018.

[3] R. Aaij *et al.*, "Test of lepton flavor universality by the measurement of the $B^0 \to D^{*-}\tau^+\nu_\tau$ branching fraction using three-prong τ decays," *Phys. Rev. D*, vol. 97, p. 072013, Apr 2018.

[4] D. Müller, M. Clemencic, G. Corti, and M. Gersabeck, "Redecay: a novel approach to speed up the simulation at lhcb," *The European Physical Journal C*, vol. 78, p. 1009, Dec 2018.

[5] R. Aaij *et al.*, "Angular analysis of $B^0 \to D^{*-}D_s^{*+}$ with $D_s^{*+} \to D_s^+\gamma$ decays," *Journal of High Energy Physics*, vol. 2021, p. 177, Jun 2021.

[6] R. Aaij *et al.*, "Measurement of the ratio of branching fractions $\mathcal{B}(\overline{B}^0 \to D^{*+}\tau^-\overline{\nu}_\tau)/\mathcal{B}(\overline{B}^0 \to D^{*+}\mu^-\overline{\nu}_\mu)$," *Phys. Rev. Lett.*, vol. 115, p. 111803, Sep 2015.

[7] R. Aaij *et al.*, "Measurement of the ratio of branching fractions $\mathcal{B}(B_c^+ \to J/\psi\tau^+\nu_\tau)/\mathcal{B}(B_c^+ \to J/\psi\mu^+\nu_\mu)$," *Phys. Rev. Lett.*, vol. 120, p. 121801, Mar 2018.

[8] F. U. Bernlochner, S. Duell, Z. Ligeti, M. Papucci, and D. J. Robinson, "Das ist der HAMMER: consistent new physics interpretations of semileptonic decays," *The European Physical Journal C*, vol. 80, p. 883, Sep 2020.

[9] D. Hill, M. John, W. Ke, and A. Poluektov, "Model-independent method for measuring the angular coefficients of $B^0 \to D^{*-}\tau^+\nu_\tau$ decays," *Journal of High Energy Physics*, vol. 2019, p. 133, Nov 2019.